

## Elevated temperature properties of Mg-12Li-Al-MgO composites

WEI Xiao-wei(魏晓伟), HUANG Qing-min(黄清民)

Department of Materials Science and Engineering, Xihua University, Chengdu 610039, China

Received 28 March 2005; accepted 26 December 2005

**Abstract:** The compressive creep of Mg-12Li-Al-MgO particulate composites was investigated, which were produced by the reaction of reinforcement materials ( $B_2O_3$ ) with Mg-12Li-Al alloy melt in the temperature range of 100–190 °C and under different compressive stress in the range of 40–70 MPa with special apparatus. The content of MgO particulates is about 0, 5%, 10%, 15%(volume fraction) in Mg-12Li-Al alloy respectively. The results reveal that the creep resistance of the particulate composites is increased with increasing the content of MgO particulates and considerable improvement in creep resistance is observed in Mg-12Li-Al-MgO composites. However, over all range of temperatures and stresses, the creep data for these composites can be correlated using an empirical equation  $\dot{\epsilon}_s = A\sigma^n \exp(-Q/RT)$ , where  $n$  is 4.93 and  $Q$  is about 78.1 kJ/mol for Mg-14Li-Al alloy and  $n$  is between 7.48 and 9.47 and  $Q$  is 111.2–137.3 kJ/mol for Mg-12Li-Al-MgO composites. The different compressive creep behavior of the composites is associated with the different material constant  $A$ . The compressive creep rate is controlled by the lattice diffusion of Li and dislocation climb.

**Key words:** Mg-12Li-Al alloy; MgO particulates;  $B_2O_3$ ; microstructure; compressive creep behavior

### 1 Introduction

Mg-Li alloys have potential for use in aerospace applications because they are exceptionally light and their specific stiffness is high[1–3]. However, there are some practical difficulties, such as poor creep behavior and microstructural instability due to the very high diffusional mobility of Li[4–6]. Major efforts have been made to evaluate the microstructure and mechanical property of Mg-Li alloys with various alloying elements at different temperatures[4–13]. New objectives in advanced aerospace applications require high specific stiffness materials that have creep resistance at elevated temperature. On the view points of lightness and high strength, some studies on Mg-Li composites were reported[13–16]. Nevertheless, the compatibility of reinforcements with molten Mg-Li alloys represents a serious problem because of the very high diffusional mobility and reactivity of Li[17]. As a result, recent attention has focused on the reaction of specific materials, such as  $B_2O_3$ , Si and ZnO, with Mg-Li alloys for production of some particulates reinforced Mg-Li composites[18]. The high temperature mechanical

properties of these particulate reinforced Mg-Li composites have been indeed improved by this method[19]. On the contrary, very few studies have focused on the high temperature creep behavior of Mg-Li-Al ( $\beta$ ) composites produced with the reaction of reinforcement materials with Mg-12Li-Al melt[19]. It was therefore considered of great interest to investigate this. Thus the objective of the present study is to establish an understanding of the effect of reinforcement particulates on the creep behavior of Mg-12Li-Al-MgO composites in terms of creep kinetics and structure.

### 2 Experimental

#### 2.1 Materials

The material investigated in this study was a commercial alloy Mg-12%Li-1%Al(mass fraction). The reaction of some  $B_2O_3$  powder with each melt of Mg-12Li-Al produces Mg-12Li-Al-MgO composites containing about 0, 5%, 10% and 15%MgO(volume fraction) particulates at 740 °C. The mixing molten Mg-12Li-Al-MgO was cast into a Y-shaped permanent mould. Then the creep specimens, 8 mm in diameter by 10 mm in gauge length, were machined from the

Y-shaped ingots. The compositions were determined by wet chemical analysis and listed in Table 1.

**Table 1** Chemical composition of alloy(mass fraction, %)

Li	Al	Na	Fe	K	Mg
12.14	0.92	0.001 6	0.015	0.002	Bal.

## 2.2 Procedure

Compressive creep test was carried out with special apparatus composed of constant pressurization, heating and temperature controller, collecting data and record devices[20]. Different test temperatures (100, 130, 160 and 190 °C) and various compressive stresses (40, 50, 60 and 70 MPa) were used. With no applied load, the specimen was completely submerged in oil. The oil bath was heated to the required test temperature and left for a few hours so that the whole assembly reached the selected test temperature. All of the tests were done in triplicate in order to obtain satisfactory precision in measuring the compressive creep deformation.

XRD analysis was performed in a Rigaku diffractometer, employing the Cu  $K_{\alpha}$  radiation, the diffraction intensity was recorded in the range of 34° to 84°(2 $\theta$ ).

Specimens for SEM(JXA-840) analysis were etched in 10% hydrochloric acid in distilled water and in 1 mL nitric acid in 75 mL ethylene glycol, and while those for transmission electron microscope (H-800) were ground and chemically polished in 1/4 nitric acid/ethanol.

## 3 Results

### 3.1 Microstructure of Mg-12Li-Al-MgO composites

The microstructures of Mg-12Li-Al-MgO composites treated with B<sub>2</sub>O<sub>3</sub> powder at 740 °C are shown in Fig.1. It can be seen that many fine particulates well distribute in the matrix of Mg-Li-Al alloy, and their size is 1-5  $\mu$ m, and the more content of MgO, the shorter the particulate spacing. XRD analysis indicates that these particulates are actually MgO, as shown in Fig.2.

### 3.2 Steady compressive creep rate

The curves of compressive creep strain versus time were obtained for various combinations of applied stress and testing temperature. From the primary creep strain, steady (or secondary) creep rates were obtained. The typical creep curves of the specimens at 100 °C and under 50 MPa are shown in Fig.3.

The steady compressive creep rate( $\dot{\epsilon}_s$ , the averaged value of three specimens) of strain, in the linear portion of the creep curve which follows the primary stage, was calculated for each test over all of the stress and the temperature range. The results are listed in Table 2, and

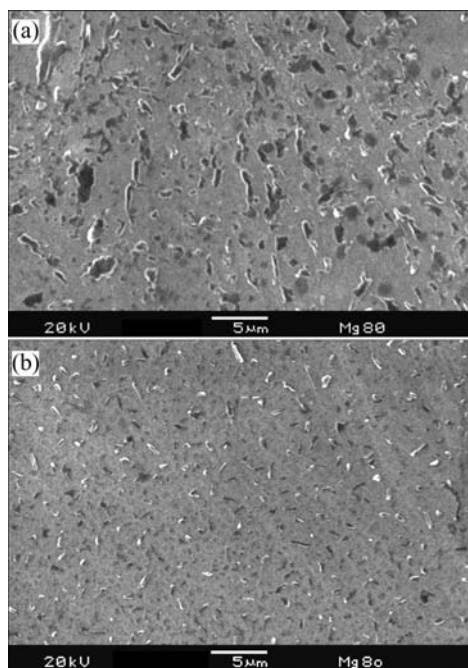


**Fig.1** SEM micrographs revealing light MgO particulates distributed in  $\beta$  phase matrix of Mg-12Li-Al alloy: (a) 10% MgO; (b) 15% MgO

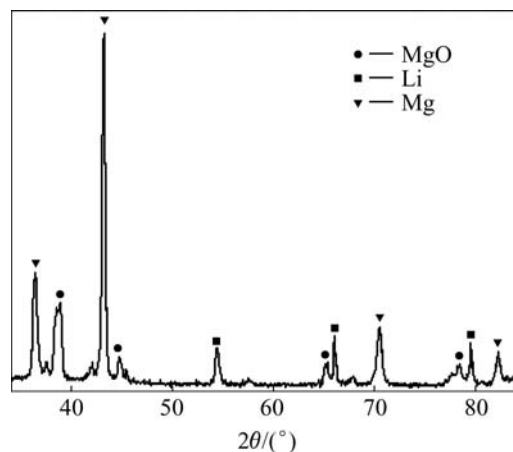


**Fig.2** XRD pattern of Mg-12Li-Al-15%MgO composites

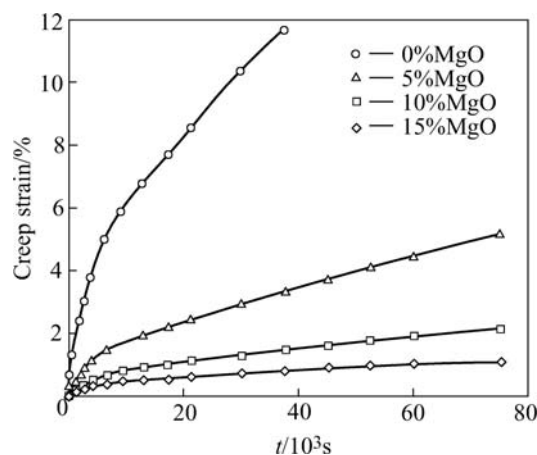


**Fig.3** Typical compressive creep curves of Mg-12Li-Al-MgO composites sample at 100 °C and under 50 MPa

plotted in forms of  $\ln \dot{\epsilon}_s$  versus  $\ln \sigma$  and  $1/T$  in Fig.4 and Fig.5. These graphs show that there is a good linear relationship between  $\ln \dot{\epsilon}_s$  and  $\ln \sigma$  or  $1/T$  for each graph under all test conditions. From Fig.5 it is observed

that the creep strength of Mg-12Li-Al-MgO composites increases as the volume fraction of MgO particulate is increased. The slopes of the curves are seen to be a function of the MgO content and stress.

**Table 2** Steady compressive creep rates of Mg-12Li-Al-MgO composites

Temperature/°C	Stress/MPa	0% MgO	5% MgO	10% MgO	15% MgO
100	40	$2.31 \times 10^{-6}$	$6.65 \times 10^{-9}$	$1.79 \times 10^{-9}$	$1.50 \times 10^{-10}$
	50	$6.11 \times 10^{-6}$	$4.09 \times 10^{-8}$	$1.61 \times 10^{-8}$	$9.16 \times 10^{-10}$
	60	$1.20 \times 10^{-5}$	$1.48 \times 10^{-7}$	$5.47 \times 10^{-8}$	$6.57 \times 10^{-9}$
	70	$3.34 \times 10^{-5}$	$3.71 \times 10^{-7}$	$2.27 \times 10^{-7}$	$3.52 \times 10^{-8}$
130	40	$9.31 \times 10^{-6}$	$3.42 \times 10^{-8}$	$8.33 \times 10^{-9}$	$2.78 \times 10^{-9}$
	50	$2.08 \times 10^{-5}$	$2.79 \times 10^{-7}$	$4.26 \times 10^{-8}$	$1.42 \times 10^{-8}$
	60	$5.48 \times 10^{-5}$	$8.23 \times 10^{-7}$	$3.11 \times 10^{-7}$	$6.65 \times 10^{-8}$
	70	$1.14 \times 10^{-4}$	$2.10 \times 10^{-6}$	$7.47 \times 10^{-7}$	$4.08 \times 10^{-7}$
160	40	$3.72 \times 10^{-5}$	$2.00 \times 10^{-7}$	$5.47 \times 10^{-8}$	$4.05 \times 10^{-8}$
	50	$8.74 \times 10^{-5}$	$1.64 \times 10^{-6}$	$5.88 \times 10^{-7}$	$2.09 \times 10^{-7}$
	60	$2.19 \times 10^{-4}$	$3.99 \times 10^{-6}$	$1.51 \times 10^{-6}$	$1.45 \times 10^{-6}$
	70	$7.74 \times 10^{-4}$	$1.45 \times 10^{-5}$	$5.26 \times 10^{-6}$	$8.71 \times 10^{-6}$
190	40	$1.19 \times 10^{-4}$	$2.07 \times 10^{-6}$	$5.01 \times 10^{-7}$	$1.27 \times 10^{-7}$
	50	$2.51 \times 10^{-4}$	$1.23 \times 10^{-5}$	$4.52 \times 10^{-6}$	$1.03 \times 10^{-6}$
	60	$8.71 \times 10^{-4}$	$4.31 \times 10^{-5}$	$1.58 \times 10^{-5}$	$5.86 \times 10^{-6}$
	70	$1.87 \times 10^{-3}$	$1.24 \times 10^{-4}$	$4.03 \times 10^{-5}$	$1.95 \times 10^{-5}$

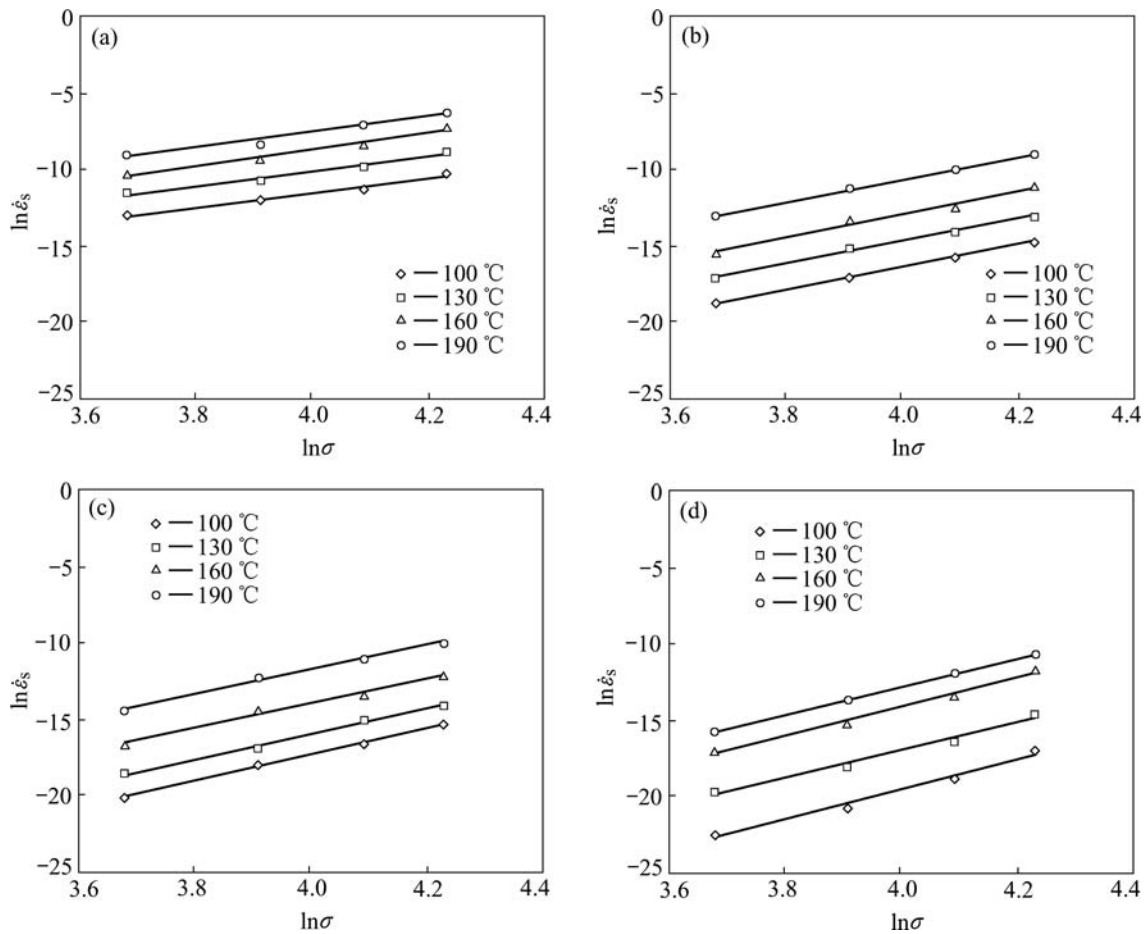


**Fig.4**  $\ln \dot{\epsilon}_s$  versus  $\ln \sigma$  for Mg-12Li-Al-MgO composites: (a) 0% MgO; (b) 5% MgO; (c) 10% MgO; (d) 15% MgO

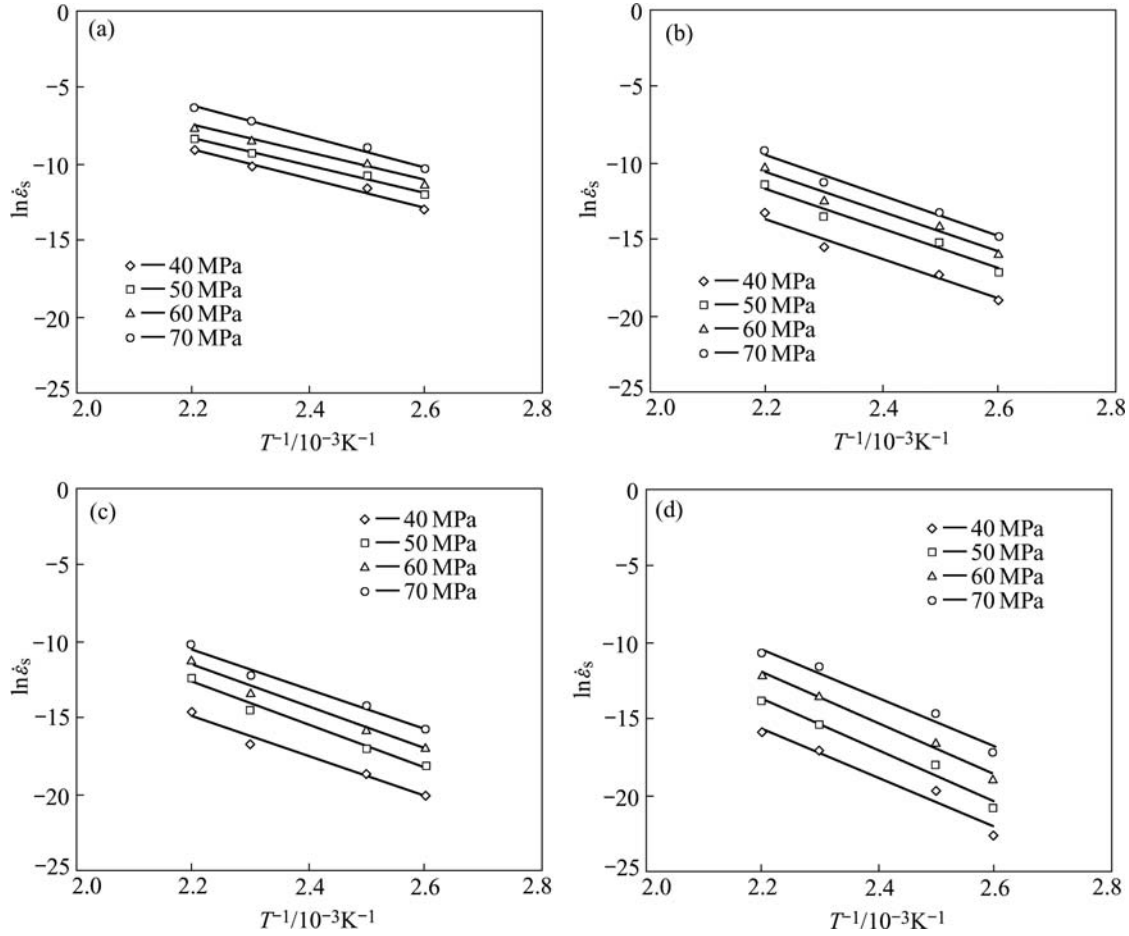


Fig.5  $\ln \dot{\epsilon}_s$  versus  $1/T$  for Mg-12Li-Al-MgO composites: (a) 0% MgO; (b) 5% MgO; (c) 10% MgO; (d) 15% MgO

**4 Discussion**

According to MISHRA et al[21], the creep data may be correlated using a simple empirical equation:

$$\dot{\epsilon}_s = A \sigma^n \exp(-Q/RT) \tag{1}$$

where  $A$  is a constant which takes into account the effects of composition and metallurgical structure,  $\sigma$  is the normal stress,  $n$  is the stress exponent,  $Q$  is an effective activation energy for creep,  $R$  is the gas constant, and  $T$  is the absolute temperature of the test. This equation implies a linear dependence of the creep strain rate on time at constant temperature and stress. Taking logarithms and rearranging, then

$$\ln \dot{\epsilon}_s = \ln A + n \ln \sigma - Q/RT \tag{2}$$

If this relationship is obeyed for the experimental materials studied here, a plot of  $\ln(\text{any fixed creep strain})$  against  $\ln(\text{stress})$  at constant temperature should be linear with a slope of  $-n$ , or a plot of the  $\ln(\text{any fixed creep strain})$  versus  $1/T$  at constant stress should be linear with a slope of  $Q/R$  over all of temperatures and stresses used.

Fig.4 and Fig.5 show that such plots for the experimental materials with  $\ln \sigma$  and with  $1/T$  as independent variable are in fact all linear with constant slopes over all of the temperatures and stresses used, respectively. The values of the exponent  $n$  and activation energy  $Q$  from these graphs are obtained and listed in Table 3. It can be seen that the average value of  $n$  is between 7.48 and 9.47 for Mg-12Li-Al-MgO composites and 4.93 closing to 5 for Mg-12Li-Al alloy respectively.

Table 3 Effect of MgO on stress exponent( $n$ ) of Mg-12Li-Al alloy

Test material	Stress exponent, $n$				Average
	100°C	130°C	160°C	190°C	
Mg-12Li-Al	4.97	5.02	4.91	4.83	4.93
Mg-12Li-Al -5%MgO	7.56	7.53	7.46	7.38	7.48
Mg-12Li-Al -10%MgO	7.93	8.65	8.52	8.31	8.35
Mg-12Li-Al -15%MgO	9.78	9.56	9.52	9.03	9.47

A stress exponent  $n$  of five is typical of a dislocation climb controlling creep rate during creep[22], in this circumstance, well-defined subgrain structures form. In 0% MgO material the primary structural parameter that affects the deformation rate is subgrain size, which

should change with applied stress, as shown in Fig.6(a). However, for the 5%, 10% and 15%MgO materials  $n$  nearly equal to 8 or more than 8 are observed. It is possible that the interparticle spacing of the MgO particulates is smaller than the equilibrium subgrain size, leading to a constant structure condition, and hence constant structure is present, leading to  $n$  values of about 8 or more than 8. The more the content of MgO particulates, the smaller the interparticle spacing of the MgO particulates. Constant structure implies that the barrier spacing to a dislocation motion (i.e. either subgrain size stabilized by particles or the interparticle space) is independent of the applied stress. A stress exponent of 8 or more than 8 is reasonable for the Mg-12Li-Al-MgO composites. This is because a constant structure can be present in the form of subgrains pinned by the MgO particulates, or by the presence of the particulates alone if they are closely spaced and effective dislocation barriers. Fig.6(b) shows that the dislocation is impeded by MgO particulates. Evidence for constant structure deformation in other particle strengthened materials, where  $n$  is equal to about 8, has been shown for a number of oxide dispersion strengthened metals[21]. Compared with 0% MgO material, the MgO composites exhibit the expected constant structure stress exponent of 8 or more than 8, indicative of the presence of a threshold stress[21]. Threshold stresses in dispersion hardened materials have often been noted and are not well understood.

The compressive creep activation energy average values achieved with Fig.5 are 111.2–137.3 kJ/mol for Mg-12Li-Al-MgO composites and about 78.1 kJ/mol for Mg-Li-Al alloy respectively, as can be seen in Table 4. The creep activation energy could not be compared with activation energy for lattice diffusion since no data appear available for Mg-Li alloys and Mg-Li-Al alloys. However, a value of lattice diffusivity ( $D_L$ ) for the Mg-Li matrix phase ( $\beta$ ) can be estimated using other low valence body-centered cubic metals (Na and Li) as guide[14]. Thus,  $D_0=0.25 \times 10^{-14}$  m<sup>2</sup>/s and  $Q_L=14.3RT_m$ . The Mg-12Li alloy melts at about 580 °C, giving a predicted activation energy for lattice diffusion of 101.41 kJ/mol. This value is less than the values of 109.9–135.2 kJ/mol noted as values for Mg-12Li-Al-MgO composites. It has been observed, however, that the activation energy for creep in many particle strengthened alloys is typically

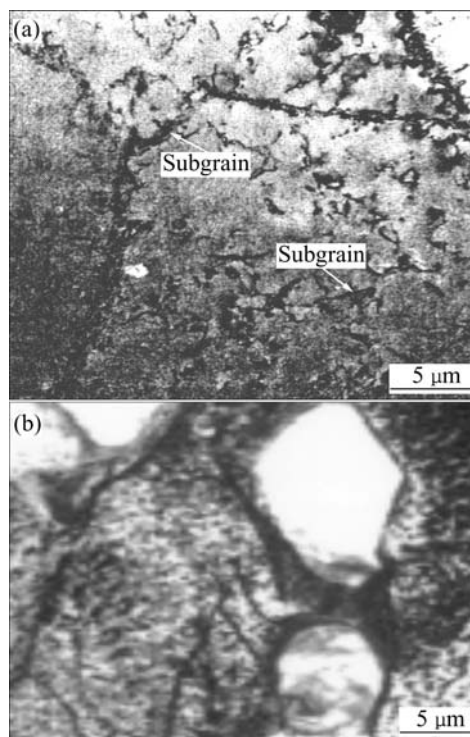


**Fig.6** Microstructures of Mg-12Li-Al-MgO composites: (a) Bright-field TEM micrograph illustrating subgrain formation during steady compressive creep deformation (at 130 °C and 50 MPa); (b) Dislocation loop round neighboring MgO particulates and dislocations near ones in composites

higher than the activation energy for lattice self-diffusion in the matrix phase. In spite of these differences it is generally believed that lattice diffusion plays an important role in these metal base materials.

When the values of  $n$  and  $Q$  are known for each Mg-12Li-Al-MgO composite and condition, the creep data may be represented parametric form by plotting values of  $\ln \dot{\epsilon}_s$  against  $[n \ln \sigma - Q/RT]$ , which should give a linear relationship with unit slope and intercept in  $\ln A$ . It can be seen that the creep data are well correlated on a line of unit slope in Fig.7. From Fig.7 the value of  $\ln A$  is 17.46 for Mg-12Li-Al alloy and 15.94, 14.29 and 11.98 for Mg-12Li-Al composites with different contents of MgO particulates, respectively. As  $\ln A$  determines the position of the line representing each experimental materials in Fig.7, which directly shows the relative creep behavior of the Mg-12Li-Al-MgO composites. It is apparent from Fig.7 that each Mg-12Li-Al-MgO

**Table 4** Effect of MgO on activation energy( $Q$ ) of Mg-12Li-Al alloy

Test material	$Q/(kJ \cdot mol^{-1})$				Average $Q/(kJ \cdot mol^{-1})$
	40 MPa	50 MPa	60 MPa	70 MPa	
Mg-12Li-Al	81.92	77.39	74.54	78.15	78.1
Mg-12Li-Al-5%MgO	107.9	111.3	112.6	108.9	111.2
Mg-12Li-Al-10%MgO	115.6	118.9	121.4	110.5	116.6
Mg-12Li-Al-15%MgO	131.6	139.6	140.2	137.7	137.3

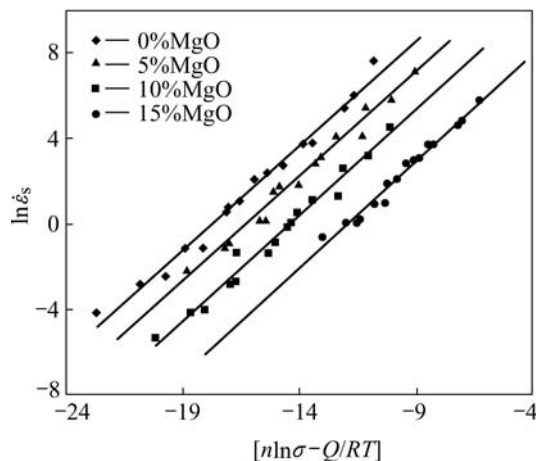


Fig.7 Relationship between  $\ln \dot{\epsilon}_s$  and  $[n \ln \sigma - Q/RT]$  for Mg-12Li-Al-MgO composites

composite has a lower creep rate than Mg-12Li-Al alloy, and that within the materials there is a clear dependence on whether containing MgO or not, a lower rate of creep being associated with the content of MgO in Mg-12Li-Al-MgO composites.

## 5 Conclusions

1) The creep rates of Mg-12Li-Al alloy and Mg-14Li-Al-MgO composites can be correlated using an empirical equation of the form:  $\dot{\epsilon}_s = A\sigma^n \exp(-Q/RT)$ , where  $n$  is 4.93 and  $Q$  is 78.1 kJ/mol for Mg-12Li-Al alloy and  $n$  is between 7.48 and 9.47 and  $Q$  is 111.2–137.3 kJ/mol for Mg-12Li-Al-MgO composites, respectively. The different compressive creep behavior of the composites was derived solely from differences in the values of constant  $A$ . The compressive creep rate was controlled by dislocation climb and the lattice diffusion of Li in the testing materials.

2) The creep resistance of Mg-12Li-Al-MgO composites increased with increasing the content of MgO particulate and considerable improvement in creep resistance was observed in Mg-12Li-Al-MgO composites, and this improvement is caused by the the fine precipitates of MgO in the alloy.

## References

[1] MATHIS K, NYILAS K, AXT A, DRAGOMIR-CERNATESCU I, UNGAR T, LUKAC P. The evolution of non-basal dislocations as a function of deformation temperature in pure magnesium determined by X-ray diffraction[J]. *Acta Materialia*, 2004, 52: 2889–2894

[2] HAFERKAMP H. Alloy development, processing and applications in magnesium lithium alloys[J]. *Materials Transactions*, 2001, 42(7): 1160–1166.

[3] CAO Fu-rong, CUI Jian-zhong, WEN Jin-lin. Deformation mechanism maps of magnesium lithium alloy and their experimental application[J]. *Trans Nonferrous Met Soc China*, 2002, 12(6): 1146–1148.

[4] YU Hua-shun, MIN Guang-hui. Effect of alloying element on Mg-Li base alloy[J]. *Rare Metal Materials and Engineering*, 1996, 52(2): 1–5. (in Chinese)

[5] MA Chun-jiang, ZHANG Di, ZHANG Guo-ding. Superlight Mg-Li alloy[J]. *Aerospace Materials & Technology*, 1998(2): 27–32. (in Chinese)

[6] LE Qi-chi, CUI Jian-hong. The past, present and future of Mg-Li alloy[J]. *Aerospace Materials & Technology*, 1997(2): 1–6. (in Chinese)

[7] YAMAMOTO A, ASHIDA T, KOUTA Y. Precipitation Mg-(4-13)%Li-(4-5)%Zn ternary alloys[J]. *Materials Transactions*, 2003, 44(4): 619–624.

[8] DROZD Z, TROJANOVÁ Z, KÚDELA S. Deformation behavior of Mg-Li-Al alloy[J]. *Journal of Alloys and Compounds*, 2004, 378: 192–195.

[9] SHEN ZE-ji, LI Yu-sheng, FENG Zhi-jun, LI De-cheng, MA Zhi-yi. New development of cast magnesium alloy[J]. *Foundry*, 2003(3): 153–156. (in Chinese)

[10] SONG G S, STAIGER M, KRAL M. Some new characteristics of the strengthening phase in  $\beta$ -phase magnesium-lithium alloys containing aluminum and beryllium[J]. *Mater Sci Eng*, 2004, A371: 371–376.

[11] LIU T, ZHANG W, WU S D, JIANG C B, LI S X, XU Y B. Mechanical properties of a two-phase alloy Mg-8%Li-1%Al processed by equal channel angular pressing[J]. *Mater Sci Eng*, 2003, A360: 345–349.

[12] CHANDRAN R, TETSUYA S, SHIGEHARU K, YO K, KAZUO M. Semi-solid forming of Mg-Li-Al-Ca light metal alloys[J]. *Japan Institute of Light Metals*, 1998, 48(1): 13–18. (in Japanese)

[13] MATSUDA A, WAN C C, YANG J M, KAO W H. Rapid solidification processing of a Mg-Li-Si-Ag alloy[J]. *Metallurgical and Materials Transactions A*, 1996, 27A(5): 1363–1370.

[14] WOLFENSTINE J, GONZALEZ-DONCEL G, SHERBY O D. Elevated temperature properties of Mg-14Li-B particulate composites[J]. *Materials Research*, 1990, 5(7): 1359–1362.

[15] MA Chun-jiang, ZHANG Di, QIN Jing-ning, WU Ren-jie. Interfacial structure of Si<sub>w</sub>/MgLiAl composites[J]. *The Chinese Journal of Nonferrous Metals*, 2000, 10(1): 23–26. (in Chinese)

[16] KUDELA S, GERGELY V, SCHWEIGHOFER A, BAUNACK S, OSWALD S, WETZIG K. The  $\delta$ -Al<sub>2</sub>O<sub>3</sub>(saffil) fibre degradation during infiltration with MgLi alloy[J]. *Materials Science*, 1994, 29: 5071–5077.

[17] MA Chun-jiang, ZHANG Di, ZHANG Guo-ding, QIN Ji-ming. Mg-Li matrix composites[J]. *Rare Metal Materials and Engineering*, 1998, 27(3): 125–129. (in Chinese)

[18] WANG Fu-zhong, LI Rong-hua, FEI Ying. Study of light Mg-Li matrix composite[J]. *Journal of Materials Science Engineering*, 2003, 21(1): 18–22. (in Chinese)

[19] YU Hua-shun, GAO Rui-lan, MIN Guang-hui. Mechanical properties and creep resistance of Mg-Li composites reinforced by MgO/Mg<sub>2</sub>Si particulates[J]. *Trans Nonferrous Met Soc China*, 2002, 12(6): 1154–1157.

[20] WEI Xiao-wei, SHEN Bao-luo, YI Yong. Compressive creep behavior of as-cast ZA27 alloy[J]. *The Chinese Journal of Nonferrous Metals*, 2003, 13(5): 1171–1174. (in Chinese)

[21] PANDY A B, MISHRA R S, MAHAJAN Y R. Steady state creep behavior of silicon carbide particulate reinforced aluminium[J]. *Acta Metall Trans*, 1992, 40A: 2045–2052.

[22] ELLSON K H, MCNELLEY T R, FOX A G. Creep behavior of Al-2.0wt Pct Li alloy in temperature rang 300 °C to 500 °C[J]. *Metallurgical Transactions*, 1993, 24A: 2001–2007.

(Edited by YUAN Sai-qian)